

# Response to tilted magnetic fields in $Bi_2Sr_2CaCu_2O_8$ with columnar defects : Evidences for transverse Meissner effect

V. Ta Phuoc, E. Olive, R. De Sousa, A. Ruyter, L. Ammor and J.C. Soret  
LEMA, CNRS- FRE 2077, Université François Rabelais, 37200 Tours, France

(Dated: 1st February 2008)

The transverse Meissner effect (TME) in the highly layered superconductor  $Bi_2Sr_2CaCu_2O_{8+y}$  with columnar defects is investigated by transport measurements. We present detailed evidence for the persistence of the Bose glass phase for  $H_{\perp} < H_{\perp c}$  : (i) the variable-range vortex hopping process for low currents crosses over to the half-loops regime for high currents; (ii) in both regimes near  $H_{\perp c}$  the energy barriers vanish linearly with  $H_{\perp}$  ; (iii) the transition temperature is governed by  $T_{BG}(H_{\parallel}, 0) - T_{BG}(H_{\parallel}, H_{\perp}) \sim |H_{\perp}|^{1/\nu_{\perp}}$  with  $\nu_{\perp} = 1.0 \pm 0.1$ . Furthermore, above the transition as  $H_{\perp} \rightarrow H_{\perp c}^+$ , moving kink chains consistent with a commensurate-incommensurate transition scenario are observed. These results thereby clearly show the existence of the TME for  $H_{\perp} < H_{\perp c}$ .

The interplay between elasticity, interactions, thermal fluctuations and dimensionality of magnetic flux lines subject to pinning, yields a large variety of vortex phases in high- $T_c$  superconductors [1]. The nature of these phases and how they depend on the pinning is far from being completely elucidated. The theory of pinning by correlated disorder, such as twin planes or amorphous columnar tracks created by heavy ions, has been considered by Nelson and Vinokur (NV) [2] and Hwa *et al* [3]. In the case of parallel tracks, NV have shown that if the applied magnetic field  $\mathbf{H}$  is aligned with the columnar defects, the low temperature physics of vortices is similar to that of the Bose glass (BG) [4], with the flux lines strongly localized in the tracks leading to zero creep resistivity. When  $\mathbf{H}$  is tilted at an angle  $\theta$  away from the column direction, the BG phase with perfect alignment of the internal flux density  $\mathbf{B}$  parallel to the columns is predicted to be stable up to a critical transverse field  $H_{\perp c}$  producing the so-called transverse Meissner effect (TME) [2, 5]. For  $\theta > \theta_c \equiv \arctan(\mu_0 H_{\perp c}/B)$ , the linear resistivity is finite resulting from the appearance of kink chains along the transverse direction as discussed in Ref. 6. Finally, above a still larger angle, the kinked vortex structures disappear and  $\mathbf{B}$  becomes collinear with  $\mathbf{H}$ . Similar scenarios apply to vortex pinning by the twin boundaries [2] and by the layered structure of the compound itself [7].

Recently, the TME in untwinned single crystals of  $YBa_2Cu_3O_7$  (YBCO) with columnar defects, has been observed using Hall sensors [8]. Previous magnetic measurements in anisotropic 3D superconductors, such as YBCO, gave support to the presence of vortex lock-in phenomena, due to pinning by the twin boundaries [9] or by the interlayers between the Cu-O planes [10]. In the case of highly layered superconductors, such as  $Bi_2Sr_2CaCu_2O_{8+y}$  (BSCCO), the lock-in transition was observed for  $\mathbf{H}$  tilted away from the layers [11], but the existence of the TME due to the pinning by columnar defects remained an open question.

In this letter, we present measurements of the electrical

properties near the glass-liquid transition in BSCCO single crystals with parallel columnar defects, as a function of  $T$  and  $\theta$  for filling factors  $f \equiv \mu_0 H_{\parallel}/B_{\Phi} < 1$ . Below a critical angle  $\theta_c(T)$ , we observe a vanishing resistivity  $\rho(J)$  for low currents. A detailed *quantitative* analysis of  $\rho(J)$  indicates that the creep proceeds via variable-range vortex hopping (VRH) at low currents due to some disorder [12], crossing over to the half-loop (HL) regime at high currents. For  $\theta > \theta_c(T)$ , the very signature of a kinked vortex structure, consistent with a commensurate-incommensurate (CIC) transition scenario in (1+1) dimensions [6], is deduced from the critical behavior of the linear resistivity. All these results clearly demonstrate that when  $\mathbf{H}$  is tilted at  $\theta < \theta_c$  away from the defects, the flux lines remain localized on columnar defects, and hence, the BG exhibits a TME.

The BSCCO single crystal was grown by a self-flux technique, as described elsewhere [13]. The crystal of  $1 \times 1 \times 0.030 \text{ mm}^3$  size with the c-axis along the shortest dimension has a  $T_c$  of 89 K, a transition width of  $\sim 1 \text{ K}$ , and was irradiated along its c-axis with 5.8 GeV Pb ions to a dose corresponding to  $B_{\Phi} = 1.5 \text{ T}$  at the GANIL (France). Isothermal  $I - V$  curves were recorded using a *dc* four-probe method with a sensitivity of  $\sim 10^{-10} \text{ V}$  and a temperature stability better than 5 mK.  $\mathbf{H}$  was aligned with the tracks using the well-known dip feature occurring in dissipation process for  $\theta = 0^\circ$ , and was tilted with an angular resolution better than  $0.1^\circ$  away from the column direction for  $f$  fixed.

Fig.?? shows a typical log-log plot of  $V/I - I$  curves obtained varying  $\theta$  for  $f = 1/3$  and  $T$  fixed below the BG transition temperature determined at  $\theta = 0^\circ$  [12]. We observe a well-defined angular crossover at an angle  $\theta_c$ . For  $\theta < \theta_c$ , data suggest that the BG phase persists. On the contrary, the existence of an Ohmic regime for  $\theta > \theta_c$  indicates a liquid vortex-like state.

We first focus on the angular range  $\theta < \theta_c$ , and we consider the scenario where the BG phase is stable. Thus, one expects that excitations of some localized vortex lines

lead to a nonlinear resistivity given by [2]:

$$\rho(J) = \rho_0 \exp(-\tilde{E}_K (J_c/J)^\mu / k_B T) \quad (1)$$

where  $\rho_0$  is a characteristic flux-flow resistivity and  $\tilde{E}_K (J_c/J)^\mu$  represents the barriers against vortex motion. This expression is predicted to hold for various regimes of different behavior as the current probes different length scales in the BG.  $\tilde{E}_K$  acts as a scaling parameter for the pinning energy and  $J_c$  is the characteristic current scale of the creep process. When the current is large enough that the growth of vortex-loops excitations of a line from its pinning track does not reach out the neighboring tracks, the HL excitations are relevant and yield an exponent  $\mu = 1$  and  $J_c \equiv J_1 = U/(\Phi_0 d)$ , where  $U$  is the mean pinning potential and  $d = \sqrt{\Phi_0/B_\Phi}$  is the mean spacing between pins. With decreasing current, size of half-loops increases with the result that some disorder in the pinning potential becomes relevant. This situation yields the VRH process characterized by  $\mu = 1/3$  and by another important current scale  $J_c \equiv J_0 = 1/(\Phi_0 g(\tilde{\mu}) d^3)$ , where  $g(\tilde{\mu})$  denotes the density of pinning energies at the chemical potential of the vortex system. One expects that both  $J_1$  and  $J_0$  are insensitive to  $H_\perp$ . We therefore consider that the only important effect of  $H_\perp$  is to lower  $\tilde{E}_K$ , according to the formula :

$$\tilde{E}_K = E_K - \epsilon^2 \Phi_0 d H_\perp \quad (2)$$

where  $E_K$  is the mean kink energy, and the energy gain due to the tilt is obtained from the isotropic result  $\Phi_0 d H_\perp$  by applying the scaling rule [Eq. (3.12)] of the Ref. 1.

We now present the following two-step method of fitting Eqs. (1) and (2) to the data, which allows to get a good understanding of the physics in our experiment. First, we plot in Fig.2 the natural logarithm of  $V/I$  versus  $\tan \theta$  for  $I$  fixed. Note that  $\tan \theta$  is here directly proportional to  $H_\perp$  since  $f$  is kept constant. A linear variation  $\ln(V/I) = M + N \tan \theta$  (expression designated below as E1) with  $M$  and  $N$  being current-dependent parameters is found for  $\theta$  varying up to  $\theta_c$  (solid lines), whereas above  $\theta_c$  data deviate from this behavior (dotted lines). This finding is another argument supporting a true angular transition at  $\theta_c$ , as suggested in Fig.???. It should be noted that we draw such a conclusion from the observation of two *independent* regimes of *different* behavior. One leads to a vanishing linear resistivity as  $\theta \rightarrow \theta_c^+$ , and the other is evidenced by probing the regions of nonlinear resistivity above and below  $\theta_c$ . Another result is that  $N \sim I^{-\mu}$  with  $\mu$  undergoing a jump from  $1/3$  to  $1$  at  $I_2 \approx 60 \text{ mA}$ . Such a current crossover is clearly visible in insert a of Fig.2 (filled symbols) where we plot together  $N$  normalized by  $I_0^{1/3}$  and  $N$  normalized by  $I_1$  versus  $I$  depending upon whether  $I$  is  $< I_2$  or  $> I_2$ , respectively. Here,  $I_0$  and  $I_1$  are two currents evaluated on the basis of the BG

model, as will be seen below. It therefrom follows that  $N_{1/3}(I) = K(I_0/I)^{1/3}$  and  $N_1(I) = K I_1/I$  where the labels  $1/3$  and  $1$  differentiate between two fits below and above  $I_2$ , respectively. In both these equations,  $K \approx 0.6$  is a dimensionless constant. It should be noted that such a crossover at  $I_2$  is clearly observed from  $V/I - I$  curves as well (see Fig.??), where a sudden increase of  $V/I$  suggesting an increasing vortex motion, occurs at  $I_2$ . Second, we plot in Fig.3 and its insert the natural logarithm of  $V/I$  versus  $I^{-1/3}$  for  $I < I_2$  and versus  $I^{-1}$  for  $I > I_2$ , respectively. We verify that the expression  $\ln(V/I) = P - Q_\mu I^{-\mu}$  (expression designated below as E2) fits very well our experimental data (solid lines) with an exponent  $\mu = 1/3$  for  $I < I_2$  and with  $\mu = 1$  for  $I > I_2$ . In E2,  $Q_\mu$  is labeled using the above convention. The result is that  $P$  is a constant (within the experimental errors), while  $Q_\mu$  depends on  $\theta$ . In Fig.4 and its lower insert, we show  $Q_{1/3}$  and  $Q_1$  versus  $\tan \theta$ , respectively. A linear variation in  $\tan \theta$  is observed consistently with expression E1. In upper insert of Fig.4, we plot together  $Q_{1/3}/I_0^{1/3}$  and  $Q_1/I_1$  versus  $\tan \theta$ . The result is that the data are superimposable onto a single straight line with slope  $\approx -0.6$  consistent with the value of  $-K$ , as may be verified by identifying the expression E1 with the expression E2.

In conclusion,  $V/I = R_0 \exp \left[ -(K' - K \tan \theta) (I_0/I)^{1/3} \right]$  is clearly observed in our experiment for  $I < I_2$  (solid lines in Fig.??) while  $V/I = R_0 \exp \left[ -(K' - K \tan \theta) (I_1/I) \right]$  is valid for data above  $I_2$  (dashed lines in Fig.??). In both fitting expressions  $K$  and  $K'$  depend on  $f$  and  $T$ . In the case of data presented in Fig.??,  $K \approx 0.6$  and  $K' \approx 0.4$ ; furthermore  $I_0 = 15 \text{ A}$  and  $I_1 = 0.4 \text{ A}$  are evaluated from BG model (see below), and  $R_0 \approx 1.1 \mu\Omega$  is five orders of magnitude lower than the normal resistance. Therefore, for  $\theta < \theta_c$  we have rather strong evidence of two separate (albeit related) vortex creep processes peculiar to a BG : the HL expansion with  $\mu = 1$  which is cut off by the crossover at  $I_2$  into the VRH process with  $\mu = 1/3$ . Moreover, we note that for each filling factor investigated in our experiment ( $f = 2/15, 1/3, 2/3$ ), we observe a *continuation* of the VRH process evidenced at  $\theta = 0^\circ$  [12]. We therefore argue that the BG phase remains stable up to a critical tilting angle  $\theta_c$ , as predicted by NV [2].

To test the accuracy of the above view, we estimate from the theory [1, 2], first the characteristic current scales, secondly the current crossover, and then the energy barriers in Eq. (1).  $J_0$  only depends on  $g(\tilde{\mu})$ , the density of pinning energies evaluated at the chemical potential of the vortex system. Although a form of  $g(x)$  is not yet available, an estimate of  $g(\tilde{\mu})$  can be done in terms of the bandwidth of pinning energies  $\gamma$ , due to the disorder, and hence  $g(\tilde{\mu}) \approx 1/(d^2 \gamma)$  so that  $J_0 \approx \gamma/(\phi_0 d)$ . Following Blatter *et al* [1],  $\gamma = t_d + \gamma_i$

where  $t_d \approx U/\sqrt{E_K/k_B T} \exp(-\sqrt{2}E_K/k_B T)$  estimates the dispersion in the pinning energies resulting from disorder in the position of tracks [2] and  $\gamma_i$  arises from some on-site randomness. We shall assume random defect radii as the main source of on-site disorder. A reasonable estimate of  $\gamma_i$  is then given by the width of the distribution of pinning energies  $\tilde{P}(U_K) = P(c_K)dc_K/dU_K$  where  $U_K$  is the binding energy of a defect with radius  $c_K$  and  $P(c_K)$  is the probability distribution of the defect radii. A realistic *pdf* is a normal law centered at  $c_0 = 45 \text{ \AA}$  with a standard deviation of  $6 \text{ \AA}$ , as shown in figure 1 of Ref. 12. Thus, using the formula  $U_K = (\phi_0^2/8\pi\mu_0\lambda_{ab}^2)\ln[1 + (c_K/\sqrt{2}\xi_{ab})^2]$  [1, 2] where  $\lambda_{ab}$  and  $\xi_{ab}$  are respectively the planar penetration depth and the planar coherence length, we determine  $U_0 = \langle U_K \rangle$  representing the energy scale for the vortex pinning. Another important energy scale corresponding to vortex positional fluctuations is  $T^* = (k_B c_0/4\xi_0 G_i)\sqrt{\ln(a_0/\xi_{ab})} (T_c - T)$  where  $G_i$  is the 2D Ginzburg number and  $a_0 = \sqrt{\phi_0/B}$  is the vortex-lattice constant.  $U_0$  and  $T^*$  completely characterize the system of vortices and columnar defects. Thus, it can be inferred  $E_K = (d/\sqrt{2}\xi_{ab}) T^* \sqrt{f(T/T^*)}$  where  $f(x) = x^2/2 \exp(-2x^2)$  accounts for entropic effects, and  $U = U_0 f(T/T^*)$ . Using appropriate parameters for BSCCO ( $\lambda_0 \approx 1850 \text{ \AA}$ ,  $\xi_0 \approx 20 \text{ \AA}$  and  $G_i \approx 0.2$ ) we estimate  $J_0 \approx 10^9 \text{ A/m}^2$  and  $J_1 \approx 2.6 \cdot 10^7 \text{ A/m}^2$  for  $f = 1/3$  and  $T = 68 \text{ K}$ . The balance between the barrier energy for the VRH process  $U_{VRH} = \tilde{E}_K (J_0/J)^{1/3}$  and the barrier for the HL regime  $U_{HL} = \tilde{E}_K J_1/J$  determines the crossover current  $J_2 = (J_1/J_0)^{1/2} J_1 = U^{3/2}/(\phi_0 d \sqrt{\gamma})$ . Thus, we have  $J_2 \ll J_1 \ll J_0$  so that the crossover between the VRH process and the HL regime takes place at  $J_2$ . Assuming uniform currents into the sample, we find  $I_2 \approx 60 \text{ mA}$  in excellent agreement with the experiment (Fig.??). A more complete quantitative evaluation of the consistency of the data with the model is obtained for different values of  $f$  and  $T$ , as well as for different values of  $d$  (insert in Fig.2). In particular, we find that the effect of  $d$  on  $I_2$  is in good agreement with the prediction  $I_2 \propto 1/d$ . Finally, evaluating  $U_{VRH}$  and  $U_{HL}$  with  $\tilde{E}_K$  from Eq. (2), we obtain using again the above usual parameters of BSCCO with  $\epsilon \approx 1/200$  that  $E_K/k_B T \approx 0.3$  and  $\epsilon^2 \phi_0 d H_\perp / k_B T \approx 0.7 \tan \theta$  for  $f = 1/3$  and  $T = 68 \text{ K}$ , which correspond to the values of our fitting parameters  $K'$  and  $K$  (see upper insert in Fig.4). Thus, the experiment is also in good agreement with the barriers  $U_{VRH}$  and  $U_{HL}$  theoretically predicted below and above  $I_2$ , respectively.

Finally, we pass on to the linear regime observed above  $\theta_c$  (see Fig. 1). For  $\theta > \theta_c$ , Hwa *et al* [6] predict on the basis of the CIC transition, the appearance of free moving chains of kinks oriented in the  $H_\perp$  direction leading to a critical behavior of the linear resistivity  $\rho \sim (\tan \theta - \tan \theta_c)^v$  characterized by an exponent  $v = 1/2$  [ $v = 3/2$ ] in  $(1+1)$  [ $(2+1)$ ] dimensions. This type

of behavior with  $v = 1/2$  is evident in Fig.5 which shows a plot of  $R/R_c$  versus  $\tan \theta - \tan \theta_c$  for different values of  $f$  (or equivalently  $H_\parallel$ ) and  $T < T_{BG}(H_\parallel, 0)$ . Here,  $R_c$  is a scaling parameter comparable to  $R_0$ , and for  $f$  fixed,  $\theta_c(T)$  is determined fitting  $R = R_c(\tan \theta - \tan \theta_c)^{1/2}$  to the data. In Fig.2, the arrow indicates  $\theta_c$  obtained in this way. The insert of the figure 5 shows  $t(H_\parallel, H_\perp) \equiv (T_{BG}(H_\parallel, 0) - T_{BG}(H_\parallel, H_\perp))/T_{BG}(H_\parallel, 0)$  as a function of  $H_\perp$  where  $T_{BG}(H_\parallel, H_\perp)$  is obtained through the inversion of  $\theta_c$  and  $T$ . It turns out that  $t(H_\parallel, H_\perp)$  is independent of  $H_\parallel$ . The solid line shown in insert is a fit to the data following  $t(H_\parallel, H_\perp) \sim |H_\perp|^{1/\nu_\perp}$  with  $\nu_\perp = 1.0 \pm 0.1$ , as recently suggested from numerical simulations [14] and observed in  $(K, Ba)BiO_3$  [15]. Moreover, such a value of  $\nu_\perp$  is excellently consistent with the result previously found using the scaling theory of the BG transition at  $H_\perp = 0$  [12].

In summary, we demonstrate from transport measurements the stability of the BG phase in BSCCO single crystal with columnar defects, when  $\mathbf{H}$  is tilted at  $\theta \leq \theta_c$  away from the column direction. We explain the critical behavior of the linear resistivity on the basis of the CIC transition of kink chains right above  $\theta_c$ , as predicted in  $(1+1)$  dimensions for one-dimensional correlated disorder. This implies that the appearance of the TME is concomitant with the vanishing of the linear resistivity at  $\theta_c$ . As a consequence, our results support the scenario for an usual BG to liquid transition in irradiated BSCCO in contrast to a puzzling two-stage BG to liquid transition recently observed in untwinned YBCO with columnar defects [8].

- 
- [1] G. Blatter et al., Rev. Mod. Phys. **66**, 1125 (1994).
  - [2] D.R. Nelson and V.M. Vinokur, Phys. Rev. B **48**, 13060 (1993).
  - [3] T. Hwa et al., Phys. Rev. Lett. **71**, 3545 (1993).
  - [4] M.P.A. Fisher et al., Phys. Rev. B **40**, 546 (1989).
  - [5] N. Hatano and D.R. Nelson, Phys. Rev. B **56**, 8651 (1997).
  - [6] T. Hwa, D.R. Nelson and V.M. Vinokur, Phys. Rev. B **48**, 1167 (1993).
  - [7] D. Feinberg and C. Villard, Phys. Rev. Lett. **65**, 919 (1990); L. Balents and D.R. Nelson, Phys. Rev. B **52**, 12951 (1995).
  - [8] A.W. Smith et al., Phys. Rev. B **63**, 064514 (2001).
  - [9] M. Oussena et al., Phys. Rev. Lett. **76**, 2559 (1996); A.A. Zhukov et al., Phys. Rev. B **56**, 3481 (1997); I.M. Obaidat et al., Phys. Rev. B **56**, R5774 (1997).
  - [10] A.A. Zhukov et al., Phys. Rev. Lett. **83**, 5110 (1999); Y. V. Bugoslavsky et al., Phys. Rev. B **56**, 5610 (1997).
  - [11] F. Steinmeyer et al., Europhys. Lett. **25**, 459 (1994); S. Kolešnik et al., Phys. Rev. B **54**, 13319 (1996).
  - [12] J.C. Soret et al., Phys. Rev. B **61**, 9800 (2000).
  - [13] A. Ruyter et al., Physica C **225**, 235 (1994).
  - [14] J. Lidmar and M. Wallin, Europhys. Lett. **47**, 494 (1999).
  - [15] T. Klein et al., Phys. Rev. B **61**, R3830 (2000).

Figure 1:  $V/I - I$  curves for tilted magnetic fields. From the right to the left  $\theta = 0, 5, 10, 15, 20, 25, 30, 35$  and  $40^\circ$ . The curved lines are a fit of the Bose glass theory to the data.

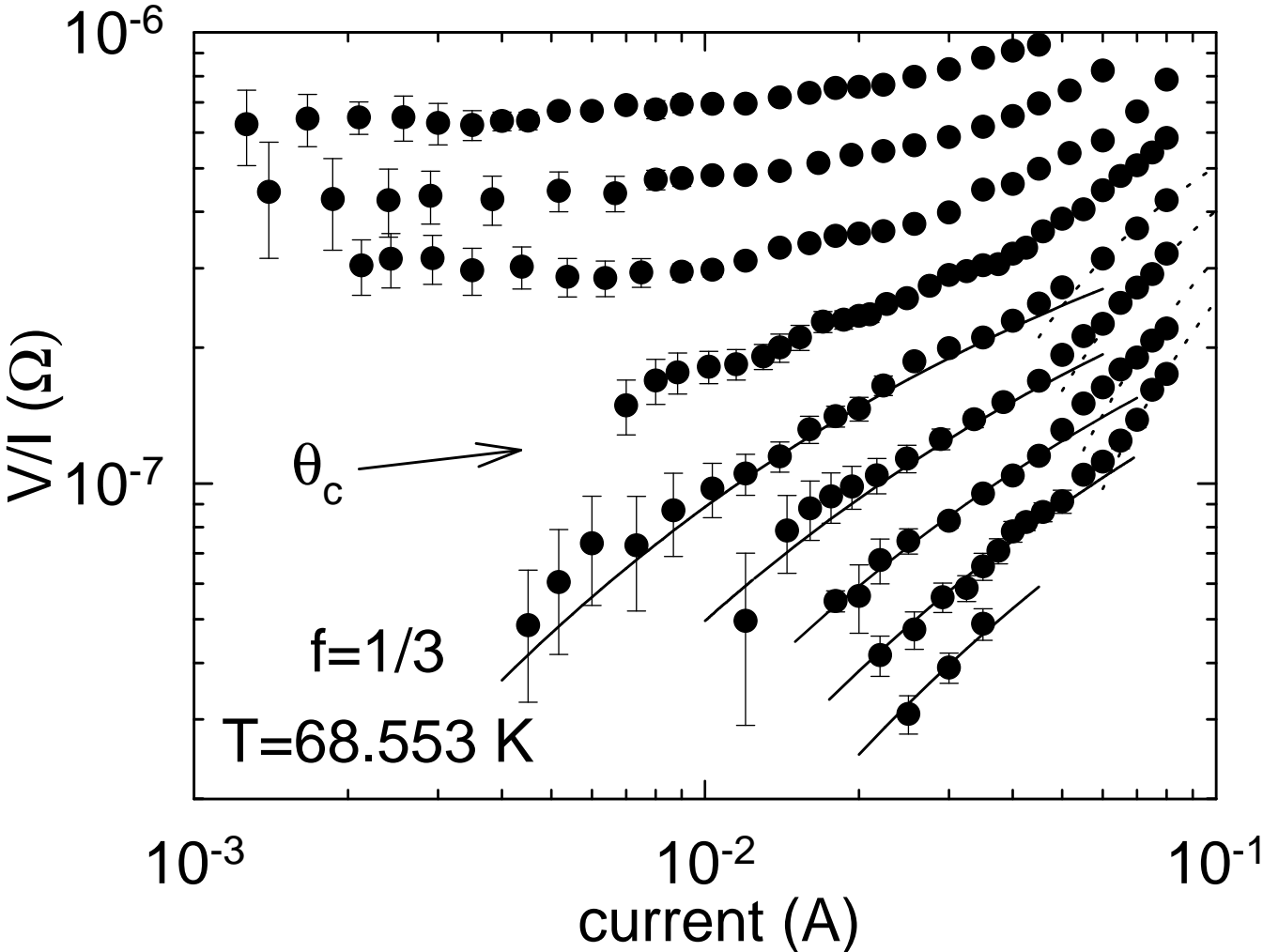
Figure 2: Angular dependence of  $\ln(V/I)$  for different  $I$ . The solid lines are a fit of  $\ln(V/I) = M + N \tan \theta$  to the data; the dotted lines are a guide for the eye. Insert:  $N/I_0^{1/3}$  vs  $I$  (left axis) and  $N/I_1$  vs  $I$  (right axis) with  $I_0$  and  $I_1$  determined from theory. (a)  $f = 1/3$  and  $T = 68.553K$  (filled symbols),  $f = 2/15$  and  $T = 69.136K$  (open symbols). (b)  $f = 1/3$  and  $T = 59.960K$  in another crystal with  $B_\Phi = 0.75 T$ . The straight lines are fits whence we obtain  $\mu = 0.33 \pm 0.05$  (solid line) for  $I < I_2$  and  $\mu = 1.0 \pm 0.1$  (dashed line) for  $I > I_2$ .

Figure 3:  $\ln(V/I)$  vs  $I^{-1/3}$  for  $I < I_2$  and  $\theta < \theta_c$ . Insert:  $\ln(V/I)$  vs  $I^{-1}$  for  $I > I_2$  and  $\theta < \theta_c$ . In both plots the lines are a fit to the data using the form  $\ln(V/I) = P - Q_\mu I^{-\mu}$  with  $\mu = 1/3$  or  $1$  according to whether  $I$  is  $< I_2$  or  $> I_2$ .

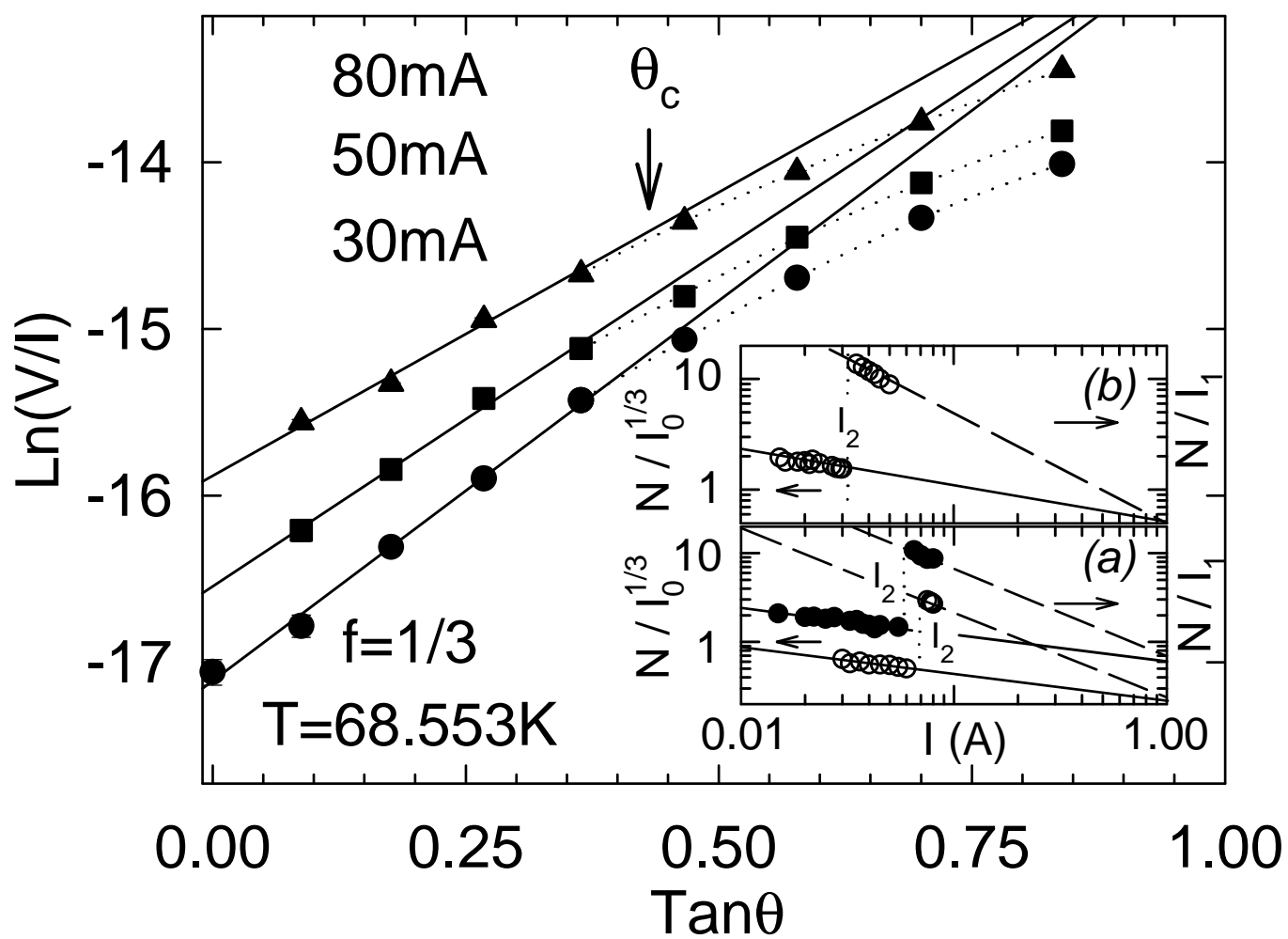
Figure 4: Angular dependence of  $Q_{1/3}$  defined in the regime  $I < I_2$  (see Fig.3). Lower insert: angular dependence of  $Q_1$  defined in the regime  $I > I_2$ . Upper insert: angular dependence of  $Q_{1/3}/I_0^{1/3}$  and  $Q_1/I_1$ . In each plot the straight line is a least-square fit.

Figure 5: Critical behavior of the linear resistance for different values of  $f$  and  $T$ . The curved line is a fit to the data using  $R = R_c(\tan\theta - \tan\theta_c)^{1/2}$  in accordance with a CIC transition scenario. Insert: angular dependence of the Bose glass transition. The solid line is a fit of  $T_{BG}(H_{\parallel}, 0) - T_{BG}(H_{\parallel}, H_{\perp}) \sim |H_{\perp}|^{1/\nu_{\perp}}$  with  $\nu_{\perp} = 1.0 \pm 0.1$  to the data, the point  $(0, 0)$  included.

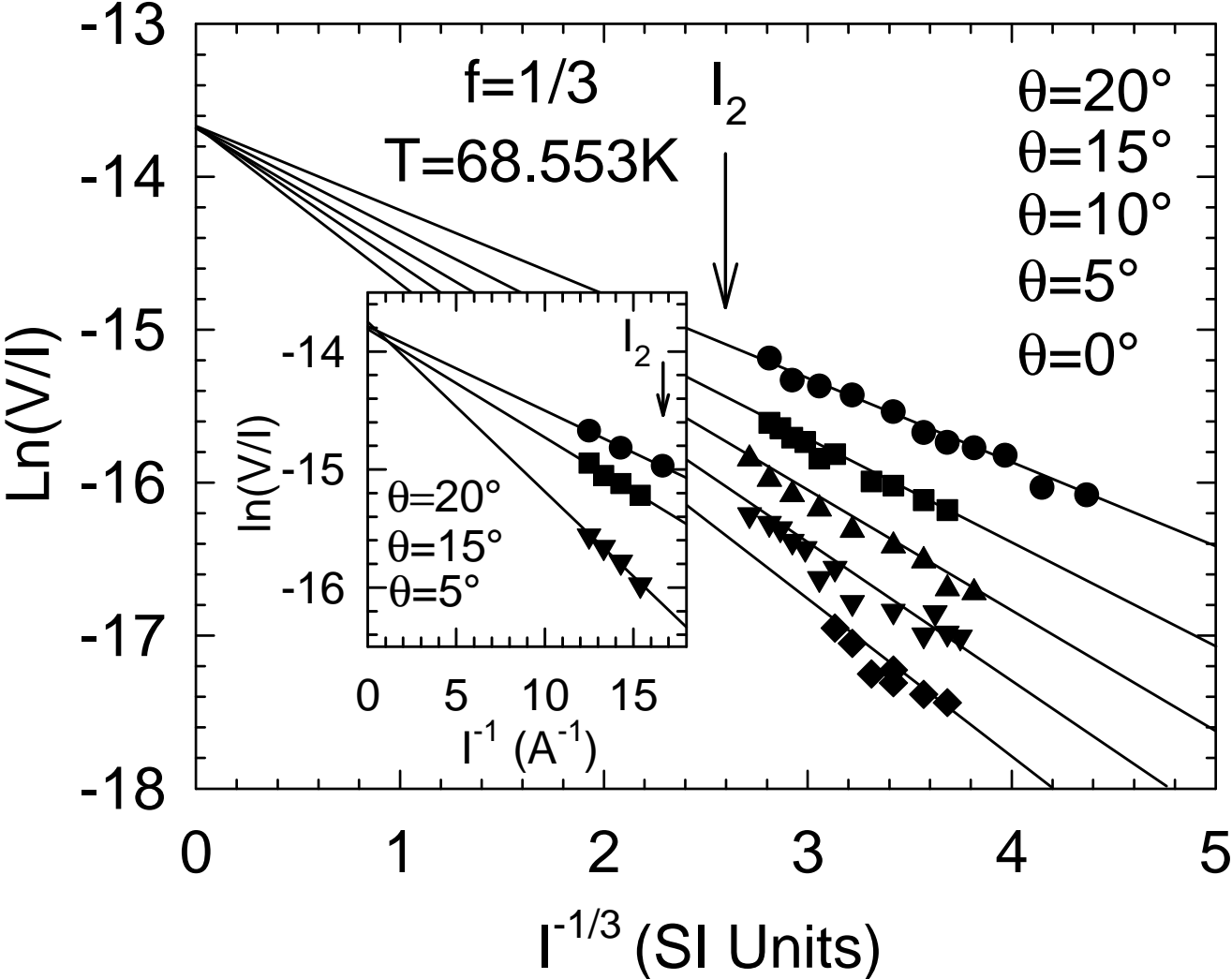
Ta Phuoc *et al.*, Figure 1



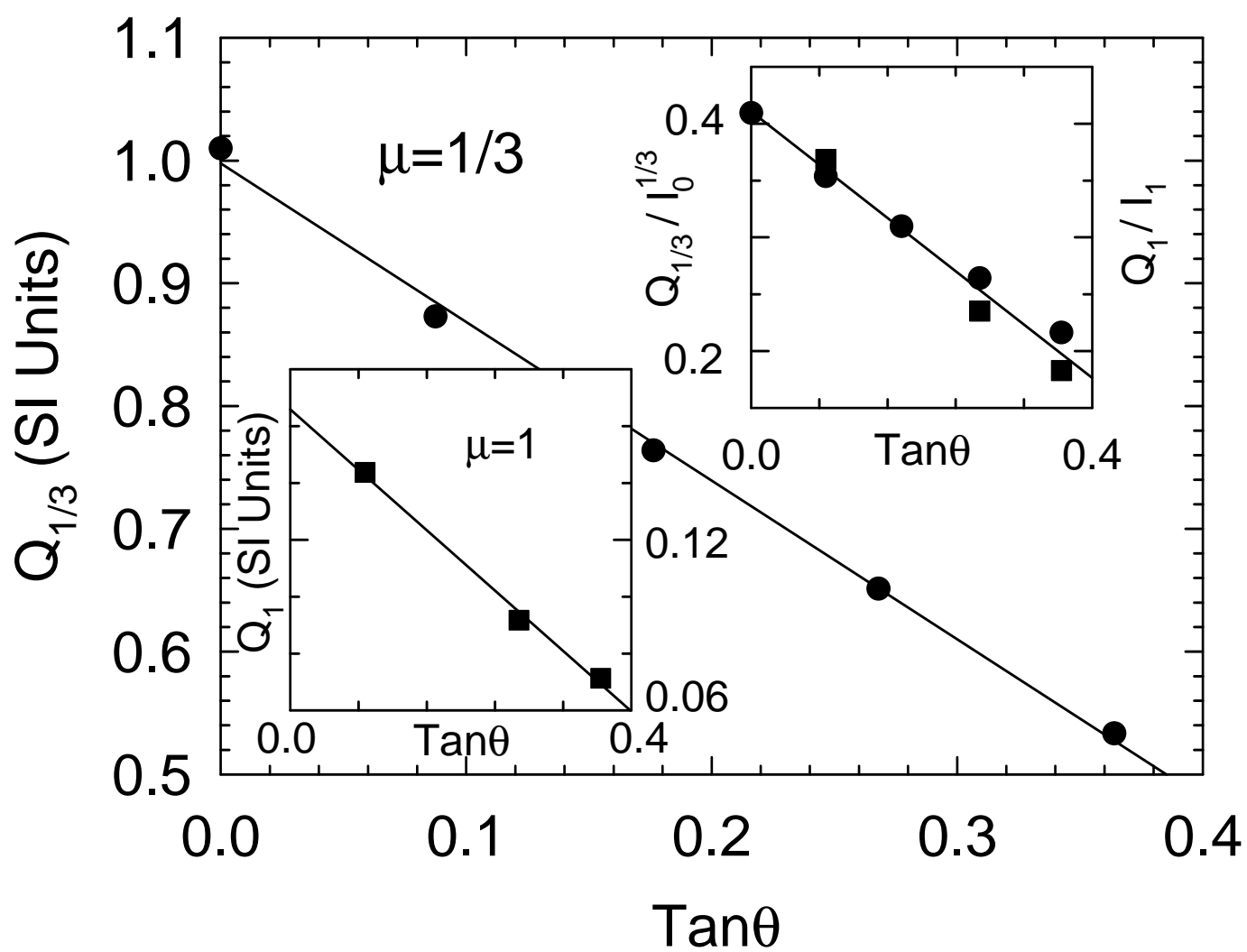
Ta Phuoc *et al.*, Figure 2



Ta Phuoc *et al.*, Figure 3



Ta Phuoc *et al.*, Figure 4



Ta Phuoc *et al.*, figure 5

